

# Porosity, Permeability, and Pore Size Distributions for Snake River Plain, Idaho Basalts: Implications for CO<sub>2</sub> Mineralization in Basalt

Robert W. Smith<sup>1,2</sup> ([smithbob@uidaho.edu](mailto:smithbob@uidaho.edu)), Travis L. McLing<sup>2,3</sup>, Ghanashyam Neupane<sup>2,3</sup>, Trevor A. Atkinson<sup>2,3</sup>, and Ram Kumar<sup>2,3</sup>  
<sup>1</sup>University of Idaho, Moscow, ID, USA; <sup>2</sup>Center for Advanced Energy Studies, Idaho Falls, ID, USA; <sup>3</sup>Idaho National Laboratory, Idaho Falls, ID, USA

Snake River Plain Basalt with natural calcite mineralization



## Introduction

CO<sub>2</sub> capture and storage in geologic formations is a recognized strategy for the mitigation of atmospheric greenhouse gas emissions in which CO<sub>2</sub> is captured and injected as a free phase (supercritical) or aqueous phase (dissolved in water) into the subsurface. Large basalt provinces such as the Snake River Plain (SRP) in southern Idaho, USA represents a formation type that has the potential to mineralize and permanently sequester gigaton quantities of CO<sub>2</sub> as carbonate minerals. However, the quantitative assessment of the capacity and rate of mineralization requires, among other things, an understanding of the release of divalent base cations (Ca, Mg, and Fe) which is a function of the reactive surface area of basalt. Commonly, geometric considerations (e.g., fracture) or B.E.T. gas adsorption are used to estimate surface areas resulting in values that differ from each other by orders of magnitude. For example, two grain size fractions of SRP basalt used in ongoing batch kinetic experiments had geometric surface areas of 8.99·10<sup>-3</sup> and 3.49·10<sup>-3</sup> m<sup>2</sup>/g compared to B.E.T. surface areas of 0.634 and 0.589 m<sup>2</sup>/g. Given that reactions rates directly scale with reactive surface area, identifying the fraction of total surface area that participates in reactions is critical.

## Methods and Results

An alternative approach to directly assess surface area is the use of mercury porosimetry which provides a simultaneous measurement of surface area and pore size distribution<sup>1</sup>. Core Laboratories, Inc. (1997) conducted a testing program of 15 samples collected from TAN-33 drill core that penetrated vertically fractured, horizontally fractured, and massive sections of SRP basalt flows (see well log) to determine:

- Pore size distribution
- Permeability to groundwater
- Porosity
- Surface area

<sup>1</sup>The Core Labs Study provided mercury intrusion as a function of discrete pressures (to a maximum of 50,000 psia) that were used to calculate pore size distribution and surface area for the basalt samples (Allen 1997).

$$r_{pore} = \frac{2\gamma \cos \theta}{p} \text{ and } S_{area} = -\frac{1}{m \cdot \gamma \cos \theta} \int_0^V p dV \approx -\frac{1}{\gamma \cos \theta} \sum \bar{p} \Delta V$$

Where  $r_{pore}$  is the pore radius,  $\gamma$  is the surface tension of mercury (0.480 N/m<sup>2</sup>),  $p$  is the mercury intrusion pressure,  $\theta$  is the contact angle (140°),  $S_{area}$  is the surface area,  $m$  is the sample mass,  $\bar{p}$  is the average pressure and  $\Delta V$  is the volume of injected mercury per unit mass of basalt.

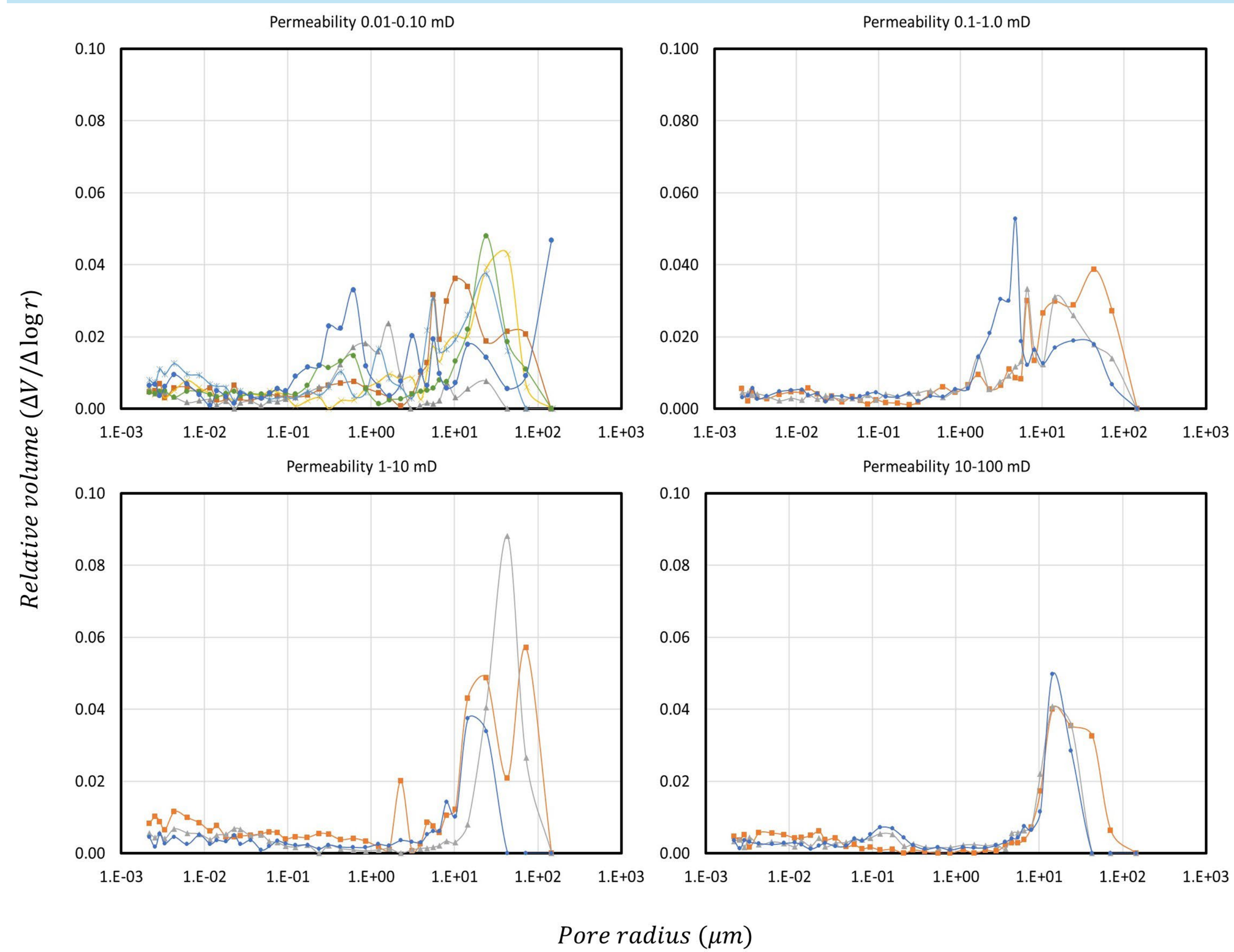


Figure 1. Pore size distribution of Snake River Plain Basalts as a function of 4 permeability ranges show that higher permeability samples are dominated by larger pore and lower permeability samples show a broader range of pore sizes.

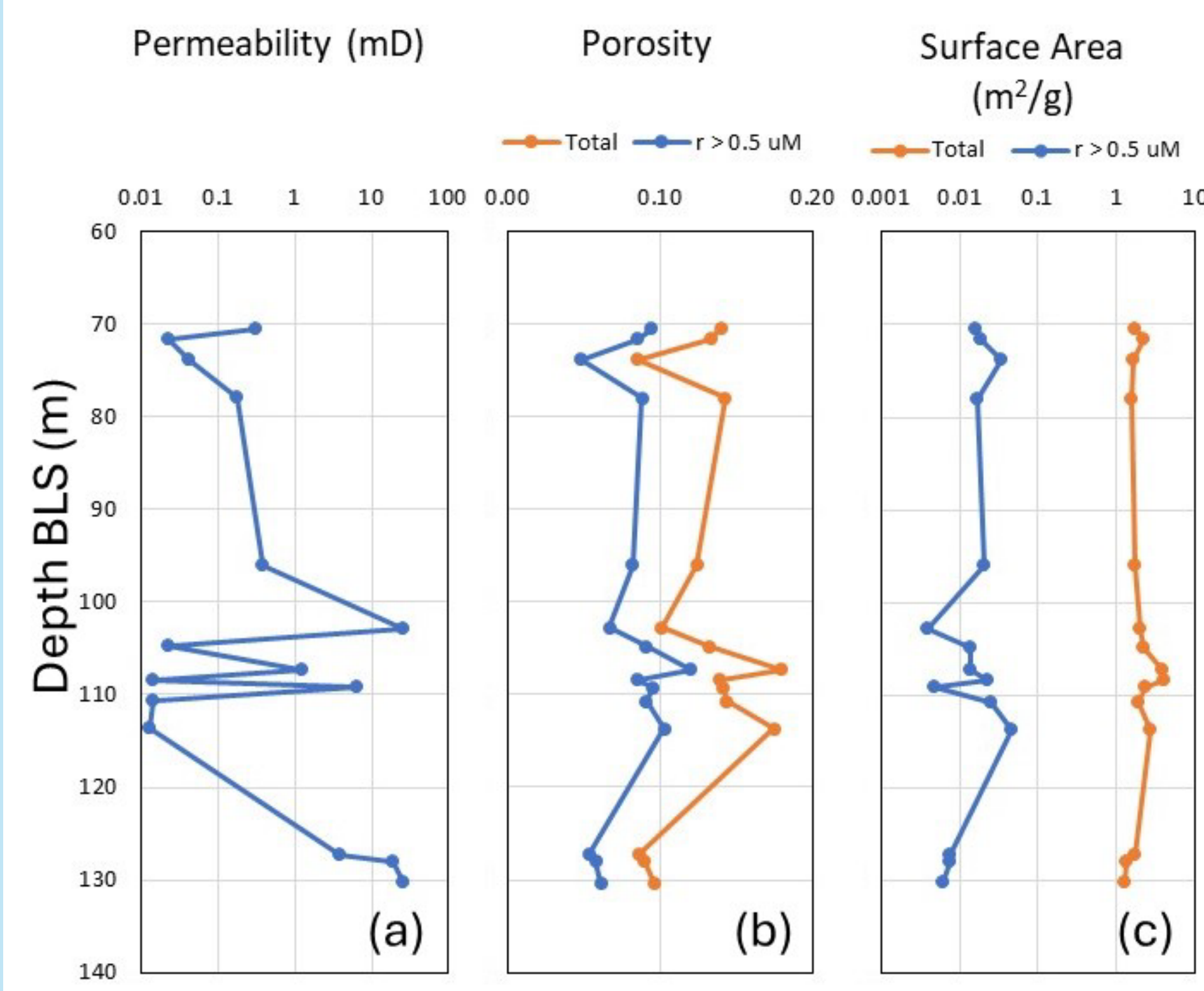


Figure 2. (a) Permeability to groundwater of Snake River Plain Basalts varied by a factor of 2,000 (range 0.013-26.1 millidarcy) and was minimally correlated ( $R^2=0.22$ , not shown) with porosity. (b) Porosity ranged from 8.5-18%, with approximately two-thirds of the porosity being associated with larger pores (greater than 1  $\mu$ m in diameter). (c) Total surface area ranged from 1.3-4.0 m<sup>2</sup>/g, with an average of 0.8% of the surface area associated with larger pores and greater than 99% of the surface area associated with pore less than 1  $\mu$ m in diameter.

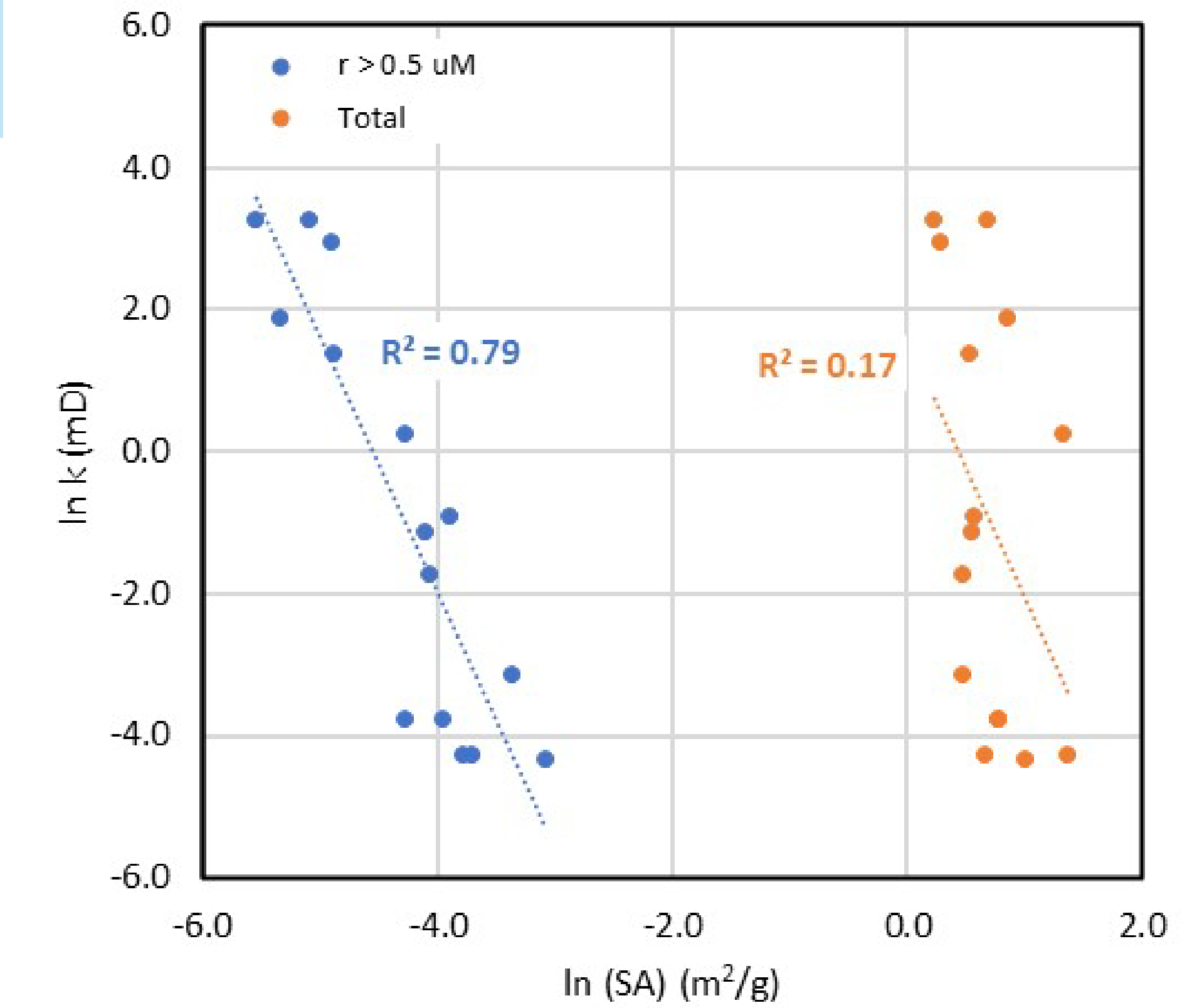


Figure 3. The permeability of Snake River Plain Basalts was more highly correlated with the surface area of larger pores ( $R^2=0.79$ ) than with the total surface area ( $R^2=0.17$ ) suggesting the small pores with large, aggregated surface area do not significantly contribute to advective transport.

## Discussion and Conclusions

Mercury porosimetry allows the assessment of the relationship of surface area to pore size distribution. We found a correlation between surface area of larger pores (>1  $\mu$ m diameter) representing ~ 0.7% of the total surface area and permeability (an indication pore interconnectedness). Using image analysis of scanning electron micrographs (2  $\mu$ m resolution) Awolayo et al. (2022) quantified the fluid-accessible mineral surface areas of a single SRP basalt sample with a B.E.T. surface area of 0.25 m<sup>2</sup>/g. Their results suggest that accessible surface area represents ~0.1% of the B.E.T. surface area. This compares to 0.1-0.9% of total surface area for pores with a diameter >2  $\mu$ m determined using Hg-porosimetry.

The observed correlation between surface area of larger pores and permeability indicates that injected CO<sub>2</sub>-rich fluids will primarily flow through higher permeability, smaller surface area (less reactive) regions in basalt formation minimizing the potential for carbonate mineralization prematurely limiting injection. It is also consistent with a two-domain conceptual model of the basalt matrix in which the long-term mineralization rate is controlled by mass transfer between a relatively non-reactive large-pore domain in which fluid flow (CO<sub>2</sub> plus water) occurs and a less mobile to stagnant highly reactive small-pore, large surface area domain.

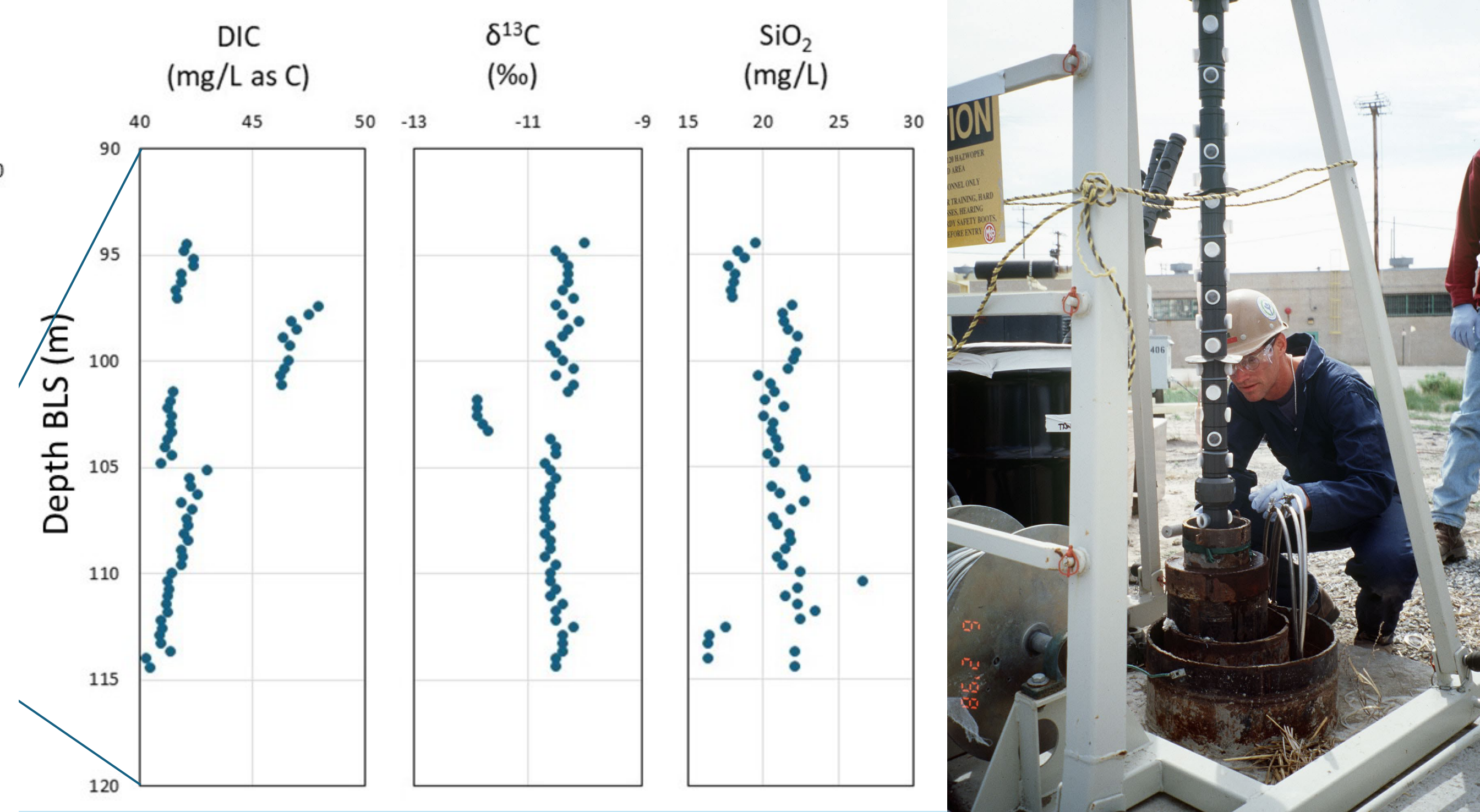


Figure 4. Vertical variations in groundwater composition for the TAN-33 well collected at a vertical resolution of 36-cm using a passive multilevel sampler (right). Groundwater compositions of (left to right) dissolved inorganic carbon (DIC),  $\delta^{13}C$ , and SiO<sub>2</sub> exhibits subtle but distinct variations that are correlated with geologic features (interflow zones, fractured flow-interiors, and unfractured flow-interiors) of the aquifer. The sharp compositional contrasts suggest that in the absence of vertical fractures there is little vertical transport. (Smith et al. 1999)

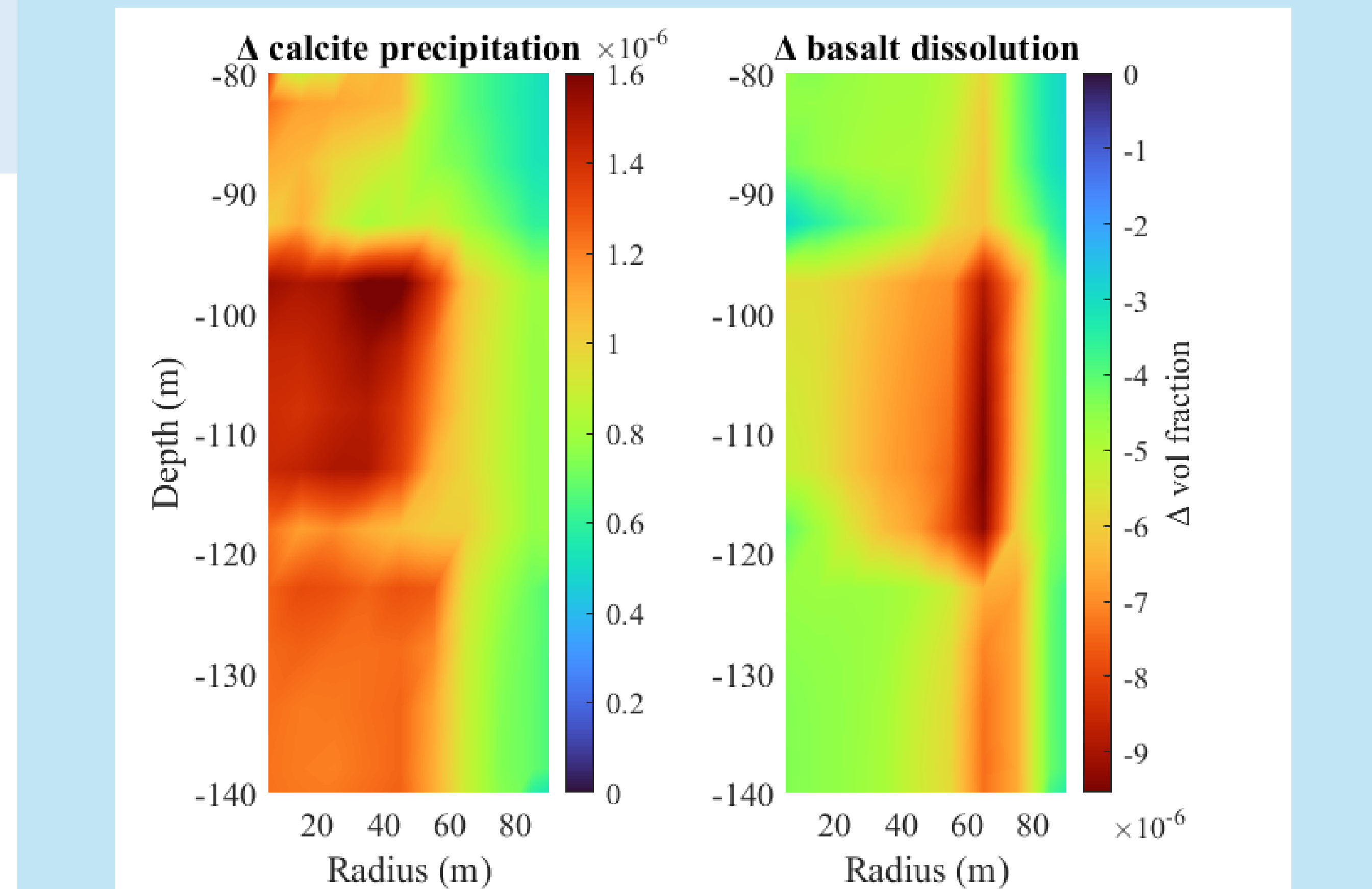
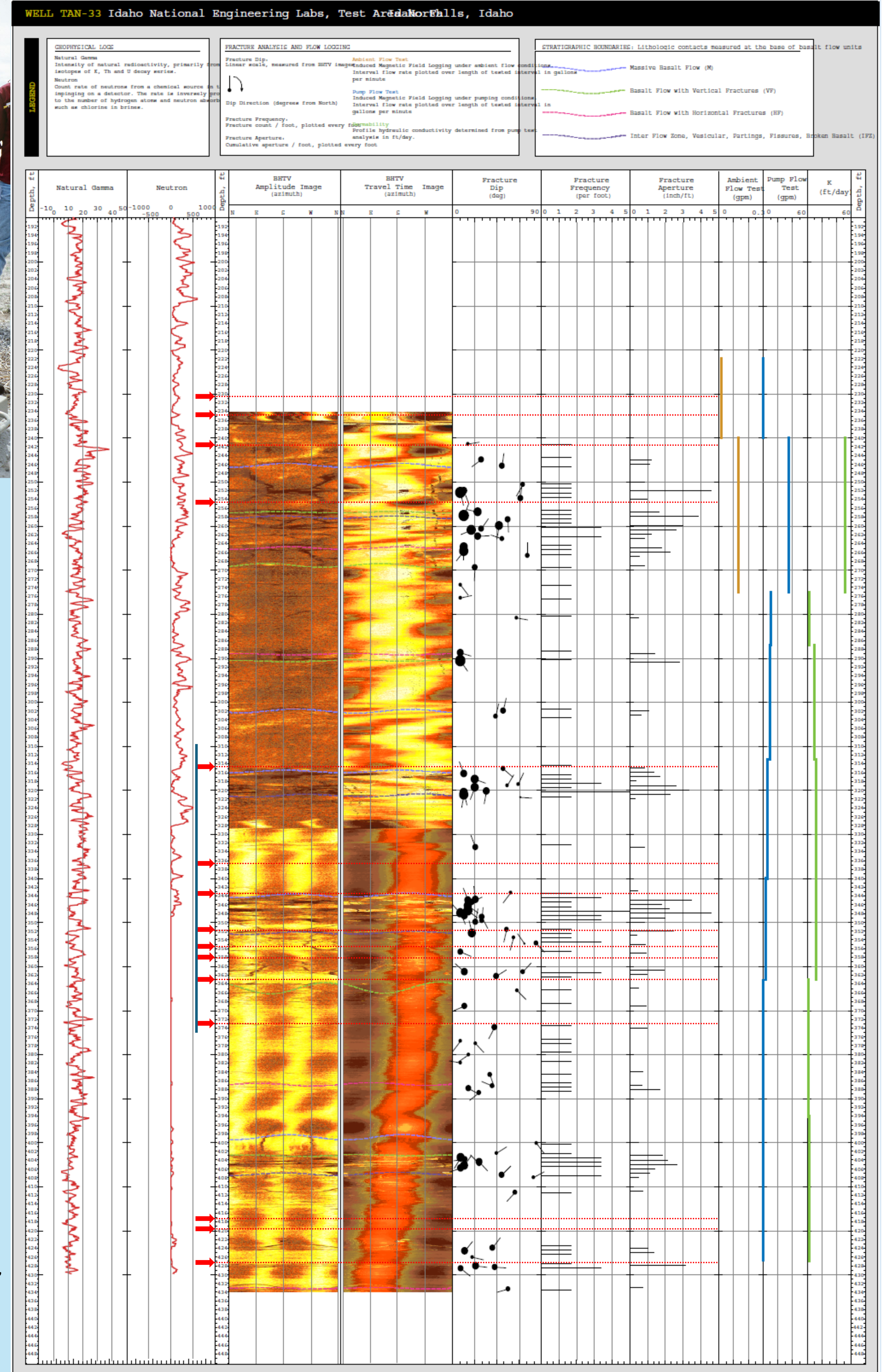


Figure 5. Reactive transport modeling results of CO<sub>2</sub> injection comparing two scenarios (total vs  $r>0.5 \mu$ m) as shown in figure 2. Differences in calcite precipitation (left) and basalt (as plagioclase) dissolution (right) are plotted in terms of volume fraction of total rock volume. Permeability, porosity, and surface areas are averaged separately for three depths 70-80 m, 90-120 m, and 120-140 m for both the cases (total and  $r>0.5 \mu$ m). A constant injection of supercritical CO<sub>2</sub> at rate of 15 kg/s is carried out for 5 years in a fully screened well (across all the layers). The magnitude of difference in mineralogical changes of calcite and plagioclase are largely due to changes in surface area. However, the color difference/depth across the three layers can be attributed to differences in their permeabilities. The total surface area simulation result in ~30% more precipitated calcite in comparison to the surface area associated with pores >1  $\mu$ m diameter.



TAN-33 Well Log. The TAN-33 well was drilled and cored as part of a study to (in part) assess recent calcite precipitation in response to microbial degradation of a Trichloroethylene (TCE) groundwater plume at Test Area North (TAN) facility at the Idaho National Engineering and Environmental Laboratory (INEL; Tobin et al. 2000). Red arrows indicate basalt sampling depths. Teal interval indicates multilevel groundwater sampling.

## References

Allen, T (1997) *Particle Size Measurement Volume 2: Surface Area and Pore Size Determination*. 5th edition, Chapman & Hall, London, UK 251 p. <https://link.springer.com/book/9780412753305>.

Awolayo AN, CT Laureijs, J Byng, AJ Luhmann, R Lauer, and BM Tutolo (2022) Mineral surface area accessibility and sensitivity constraints on carbon mineralization in basaltic aquifers *Geochimica et Cosmochimica Acta* **334**:293-315. <https://doi.org/10.1016/j.gca.2022.08.011>.

Core Labs (1997) *Advanced Core Analysis Test Program*. File DAL-97003 Core Laboratories, Inc., Carrollton, TX.

Smith RW, FS Colwell, RM Lehman, TL McLing, and JP McKinley (1999) Vertical Variations in Composition for TCE Contaminated Groundwater at the Test Area North (TAN), Idaho National Engineering and Environmental Laboratory, Idaho (abs.). 4<sup>th</sup> International Symposium on Subsurface Microbiology, August 22-27, 1999, Vail, CO.

Tobin, KJ, FS Colwell, TC Onstott, and RW Smith (2000) Recent calcite spar in an aquifer waste plume: a possible example of contamination driven calcite precipitation. *Chemical Geology* **169**(3-4):449-460. [https://doi.org/10.1016/S0009-2541\(00\)00220-5](https://doi.org/10.1016/S0009-2541(00)00220-5).